

HELIOSEISMOLOGY: Oscillations as a Diagnostic of the Solar Interior

Franz-Ludwig Deubner

Institut für Astronomie und Astrophysik, Universität Würzburg,
Würzburg, Federal Republic of Germany

Douglas Gough

Institute of Astronomy and Department of Applied Mathematics and
Theoretical Physics, University of Cambridge, Cambridge, England

1. INTRODUCTION

The detection of a rich spectrum of resonant oscillations of the Sun in the course of the past decade is making it possible to investigate important basic properties of the solar interior. The term “helioseismology” is now widely used to describe this new field of research.

About ten years after the first observation of the “five-minute oscillations” by Leighton and his coworkers (115, 115a) and by Evans & Michard (65), Ulrich (151) presented a sound theoretical description of the phenomenon. A similar, though less complete, theory was advanced by Leibacher & Stein (113). The oscillations are standing acoustic waves, most of which are trapped beneath the photosphere in the upper layers of the convection zone. Their amplitudes are low, so linearized theory is valid. Ulrich, and subsequently Ando & Osaki (1), predicted sequences of eigenfrequencies that depend on the horizontal wavelength of the oscillations. Five years later, the theory was confirmed by the observations of Deubner (44).

At about the same time, new observations with different kinds of instruments (13, 97, 141) revealed the existence of other oscillations at periods (20–60 min, 160 min) quite different from the familiar five-minute range. These findings marked the beginning of a new phase of interest in hydrodynamical phenomena deep in the interior of the Sun.

In this article we outline the most recent advances in the diagnostic aspects of the subject. A more detailed account of the early development of helioseismology may be found in a number of other reviews (45, 46, 73, 94, 148). We begin by discussing the conditions that must be satisfied for low-amplitude waves to be able to propagate, to make it apparent where in the Sun the waves are trapped, and to display the aspects of the solar structure that are predominantly responsible for determining the frequencies. Our approach is somewhat different from previous discussions, and thus we hope it will be useful even to readers who are already familiar with the subject. We then summarize briefly the observational techniques and review the major areas where progress is being made, discussing in turn the modes of high, low, and intermediate degree. Interpretations of limb observations are still uncertain, and we have refrained from presenting a detailed critique.

The current main product of helioseismology is a theoretical model of the spherically symmetrical component of the Sun. Oddly enough, that model is quite similar to the predictions of so-called standard evolution theory and suggests that the simplifying approximations in that theory do not appear to introduce severe errors in the basic hydrostatic structure of the star. It also reinforces the difficulties already encountered in explaining the low observed neutrino flux. However, there are systematic discrepancies between the observed solar oscillation frequencies and the eigenfrequencies of the best-fitting theoretical model that have not yet been eliminated. Therefore, one must treat with caution any claim that the model is certainly a close approximation to reality.

In principle, the fine structure of the oscillation spectrum should enable us to set bounds on deviations from spherical symmetry. These can be caused by rotation, large-scale magnetic fields, and convection. Already there are reports in the literature of several preliminary investigations, but few firm conclusions have yet been drawn.

2. RESONANT CAVITIES IN THE SUN

A linear normal mode of oscillation can be regarded as a standing wave resulting from the interference between oppositely directed propagating waves. The interference pattern has the following mathematical form with respect to spherical polar coordinates (r, θ, ϕ) :

$$\xi(r, \theta, \phi, t) = \text{Re}\{\Xi(r)P_l^m(\cos \theta)_{\sin}^{\cos} m\phi e^{i\omega t}\}, \quad 2.1$$

where ξ is the vertical component of the fluid displacement ξ , and P_l^m is the associated Legendre function. For any given *degree* l , there are many possible eigenfunctions Ξ . These are labeled with an integer n , called the

order of the mode (see Appendix). Broadly speaking, n measures the vertical component of the wave number, and l measures the horizontal component.

To a first approximation the Sun can be considered to be spherically symmetrical. Consequently, all orientations of the coordinate axis are equivalent. The eigenfrequencies ω cannot, therefore, depend on the azimuthal order m , for m , which measures the number of nodes on the equator, depends on the choice of coordinates. There are two sequences of modes: acoustic or p modes, for which the principal restoring force is provided by pressure fluctuations; and gravity or g modes, for which the restoring force is buoyancy.

Conditions permitting the propagation of acoustic-gravity waves have been reviewed before (e.g. 41, 114, 148, 149, 155). If the wavelength is much less than the solar radius, the local effects of spherical geometry on the dynamics can be ignored. Then the equations of motion for adiabatic oscillations can be reduced in the manner chosen by Lamb (110), leading to

$$\Psi'' + K^2 \Psi = 0, \quad 2.2$$

where $\Psi = \rho^{1/2} c^2 \operatorname{div} \xi$, ρ and c are the density and sound speed of the equilibrium state, and a prime denotes differentiation with respect to r . Perturbations to the gravitational potential have been ignored. The vertical component of the local wave number K is given by

$$K^2 = \frac{\omega^2 - \omega_c^2}{c^2} + \frac{l(l+1)}{r^2} \left(\frac{N^2}{\omega^2} - 1 \right), \quad 2.3$$

where

$$\omega_c^2 = \frac{c^2}{4H^2} (1 - 2H'), \quad 2.4$$

H being the density scale height, and

$$N^2 = g \left(\frac{1}{H} - \frac{g}{c^2} \right) \quad 2.5$$

is the square of the buoyancy (Brunt-Väisälä) frequency; g is the magnitude of the acceleration due to gravity. Equation 2.2 is a good approximation except near $r = 0$, where curvature effects are important. However, as is evident from the discussion that follows, aside from low-order modes of low degree, only modes with $l \ll n$ penetrate sufficiently close to the center of the Sun for the errors introduced by the approximation to have a significant effect on the solutions.

For the solutions to (2.2) to be wavelike, it is necessary that $K^2 > 0$. It can be seen immediately that for spherically symmetrical modes ($l = 0$), this occurs only when ω exceeds the critical frequency ω_c , which is a generalization of Lamb's (109) acoustical cutoff frequency. For nonradial

modes it is convenient to rewrite Equation 2.3 in the form

$$c^2 K^2 = \omega^2 \left(1 - \frac{\omega_+^2}{\omega^2}\right) \left(1 - \frac{\omega_-^2}{\omega^2}\right), \quad 2.6$$

where

$$\omega_{\pm}^2 = \frac{1}{2}(S_l^2 + \omega_c^2) \pm [\frac{1}{4}(S_l^2 + \omega_c^2)^2 - N^2 S_l^2]^{1/2}. \quad 2.7$$

Here,

$$S_l = [l(l+1)]^{1/2} \frac{c}{r}, \quad 2.8$$

which is sometimes called the Lamb frequency. It follows from Equation 2.6 that $K^2 > 0$ either when ω_{\pm}^2 are complex or when ω_{\pm}^2 are real and (a) $\omega^2 > \omega_-^2$ and $\omega^2 > \omega_+^2$ or (b) $\omega^2 < \omega_-^2$ and $\omega^2 < \omega_+^2$.

The critical frequencies ω_+ and ω_- are plotted in Figure 1 for a standard solar model. The horizontal lines represent modes; they are continuous in the propagating regions and dashed in the evanescent regions where neither of the conditions (a) or (b) is satisfied. It is evident that there are several regions in the Sun within which modes can be trapped.

Eigenfrequencies can easily be estimated for high-order modes, for which K^{-1} is typically much smaller than the range (r_1, r_2) of a cavity within which $K^2 > 0$. Barring accidental resonances, which would permit the mode to have high amplitude in two cavities at once, the condition for a normal mode is essentially that an integral number (n) of half wavelengths fit between r_1 and r_2 . Thus

$$\int_{r_1}^{r_2} K \, dr = \omega \int_{r_1}^{r_2} \left[\left(1 - \frac{\omega_+^2}{\omega^2}\right) \left(1 - \frac{\omega_-^2}{\omega^2}\right) \right]^{1/2} \frac{dr}{c} \simeq (n + \varepsilon)\pi, \quad 2.9$$

where the phase ε accounts for the fact that rather than vanishing at $r = r_1$ and $r = r_2$, the wave amplitude matches onto decaying solutions outside the cavity.

In the deep interior of the Sun, S_l^2 is usually rather greater than ω_c^2 and N^2 , and therefore $\omega_+ \approx S_l$ and $\omega_- \approx N$. This permits us to associate conditions (a) with acoustic modes: waves can propagate vertically provided the horizontal phase speed $\omega r/l$ does not exceed c . The vertical wave number K is influenced by buoyancy through the term $1 - N^2/\omega^2$, causing a reduction of the eigenfrequencies below what one would expect from a pure acoustic mode.

An asymptotic expression for ω when $n/l \gg 1$ has been derived by Vandakurov (156) and extended by Tassoul (150):

$$\omega_{n,l} \sim 2\pi(n + \frac{1}{2}l + \varepsilon_p)v_0 + \delta_{n,l}, \quad 2.10$$

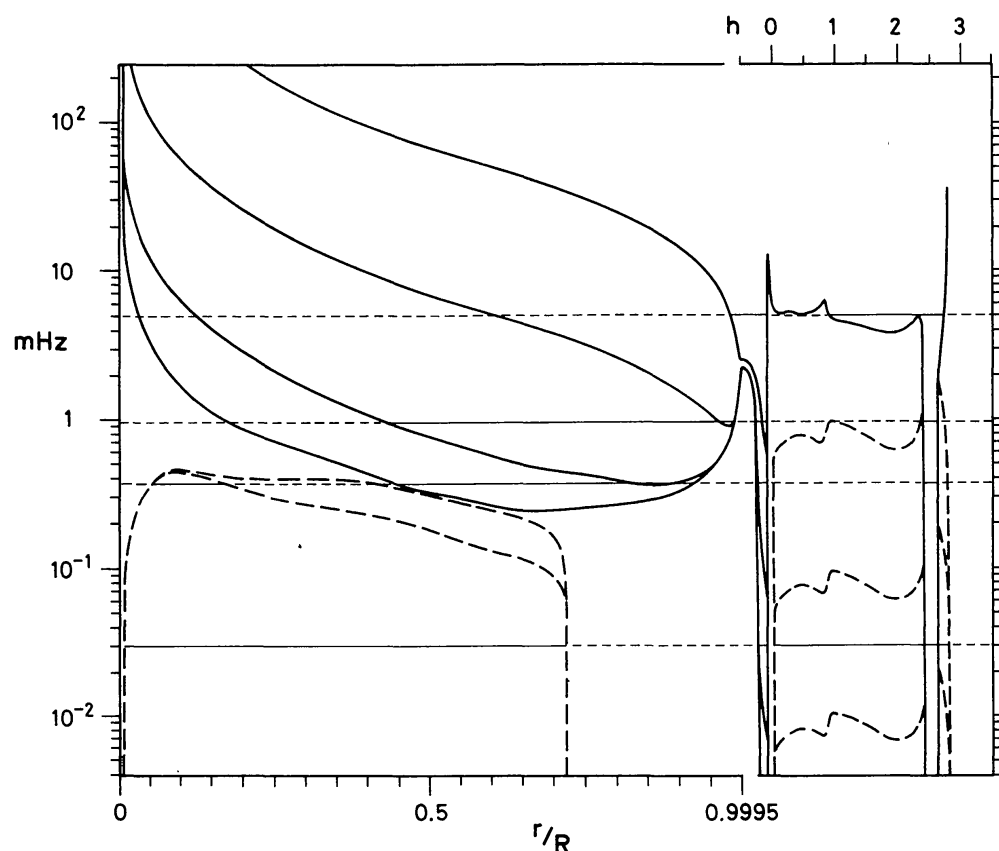


Figure 1 Propagation diagram for a model of the Sun, computed from Christensen-Dalsgaard's (23a) solar Model 1 beneath the photosphere and the temperature-optical depth relation of the Harvard-Smithsonian reference atmosphere (70b) above the photosphere. The corona is not included. Solid curves represent $\omega_+/2\pi$, and dashed curves $\omega_-/2\pi$, in the regions where the critical frequencies ω_{\pm} are real. Propagation at any frequency is possible where ω_{\pm} are complex. The lower abscissa scale extends to $r/R = 0.9995$; beyond that value, the scale is expanded by a factor of 100, and the scale is indicated on the upper boundary of the diagram: The independent variable is the height h above the photosphere measured in units of $10^{-3} R$. The curves ω_{\pm} are for $l = 1, 5, 50$, and 500 . In all cases, ω_{\pm} are increasing functions of l at fixed r/R , which permits the identification of the curves: In the interior the ω_- curves for $l = 5$, $l = 50$, and $l = 500$ are essentially indistinguishable, as are all four ω_+ curves in the atmosphere, where $\omega_+ \simeq \omega_c$. The thin horizontal lines represent normal modes; they are continuous in zones of propagation and dashed in evanescent regions. The lowest-frequency mode is a high-degree ($l \gtrsim 25$) g mode. Its amplitude is likely to be substantial in either the interior or the atmosphere, but not both. The next mode represents $g_1(l = 1)$, which has the character of a p mode in its outer zone of propagation. The third mode is $p_4(l = 5)$, which is a simple p mode confined to a single region of propagation. The highest-frequency mode is $p_6(l = 500)$; because the evanescent regions are thin, the mode could have a substantial amplitude both in the photosphere and in the chromosphere.

where

$$\delta_{n,l} = -2\pi v_0 \frac{\alpha l(l+1) - \beta}{n + \frac{1}{2}l + \varepsilon_p}, \quad 2.11$$

$$v_0 = \left(2 \int_0^R \frac{dr}{c} \right)^{-1}, \quad 2.12$$

and R is the radius of the Sun. Here $\varepsilon_p = \frac{1}{2}(\bar{\mu} + \frac{1}{2})$, where $\bar{\mu}$ is an effective polytropic index near $r = r_2$, and α and β are other constants that depend on the equilibrium state. In this limit, $r_1 \sim 0$ and $r_2 \sim R$, and the leading term of (2.10) follows immediately from Equation 2.9, except that l is replaced by $\sqrt{[l(l+1)]}$; an approximation to the remaining term is also given by Equation 2.9, and this is asymptotically correct when $l \gg 1$. When l is small, a more careful treatment that takes into account the curvature terms omitted from Equation 2.2 must be undertaken. Notice that the asymptotic frequencies are roughly uniformly spaced.

As $l/n \rightarrow \infty$, Equation 2.9 reduces to

$$\frac{n + \varepsilon}{\omega} \sim \frac{1}{\pi} \int_{r_1}^{r_2} \left(1 - \frac{k^2 c^2 + \omega_c^2}{\omega^2} \right)^{1/2} \frac{dr}{c}, \quad 2.13$$

where $k = [l(l+1)]^{1/2} R^{-1} \simeq l R^{-1}$ is the horizontal component of the wave number at the solar surface. The modes are confined near the surface, penetrating to a depth of about $2\Lambda(n + \varepsilon)k^{-1}$, where Λ is a constant of order unity that depends on the manner in which c^2 varies with depth. Approximating the surface layers by a polytrope of index μ yields a constant gradient $G \equiv -dc^2/dr$, provided the adiabatic exponent γ can be assumed constant. Then $\Lambda = 1$, and Equation 2.13 reduces to

$$\omega^2 \sim \frac{2(n + \varepsilon)\gamma}{\mu + 1} gk = 2(n + \varepsilon)Gk. \quad 2.14$$

The plane-parallel polytrope can actually be treated exactly (e.g. 23, 73, 74) by extending the analyses of both Lamb (110), who considered acoustic waves in a shallow polytropic layer, and Spiegel & Unno (145), who considered convective modes in a deep layer. The result has the same form as (2.14) when $n \gg 1$, with $\varepsilon = \frac{1}{2}\mu$.

Conditions (b) describe g modes. The buoyancy frequency N is the frequency of a fictitious, adiabatically vertically oscillating fluid parcel that does not displace, and remains in pressure equilibrium with, its environment. In practice there is not time to reach perfect pressure balance, and there is an acoustic modification, which increases with increasing $\omega/(kc)$.

Moreover, the environment must be displaced sideways to make way for the parcel, which effectively increases the inertia of the fluid and reduces ω . As $l \rightarrow \infty$ at fixed n , the motion becomes nearly vertical and the latter effect vanishes; ω increases to the maximum value of N , but now the mode is severely confined within the small cavity in the vicinity of this maximum (23). Moreover, the decay of the amplitude away from the edges of the propagating regions is rapid, because the opposing influences of motions separated horizontally by half a wavelength λ largely cancel beyond a radial distance of about λ into the evanescent region. Hence, high-degree internal gravity modes have very low amplitude in the photosphere and are therefore difficult to detect (see also 25, 60). As $n \rightarrow \infty$ at fixed l , Equation 2.9 yields

$$\omega^{-1} \sim (n + \varepsilon)\pi[l(l+1)]^{1/2} \left(\int_{r_1}^{r_2} \frac{Ndr}{r} \right)^{-1} \equiv \frac{(n + \varepsilon)P_0}{2\pi[l(l+1)]^{1/2}}, \quad 2.15$$

indicating that the oscillation periods are asymptotically uniformly spaced. Further details and extensions of the high-order asymptotic relations are given in (111, 150, 156, 164) and the references therein. The results have the form (2.15), with $r_1 = 0$, r_2 equal to the radius of the base of the convection zone, and $\varepsilon = \frac{1}{2}l + \varepsilon_g$ provided $N^2 > 0$ in the core; the value of the constant ε_g depends on the manner in which the convection zone matches onto the radiative interior.

Equation 2.2 does not apply to f modes, whose character is clear when $l \gg 1$. Then they are essentially surface gravity waves, satisfying $\Psi = 0$. The displacement amplitude is proportional to $\exp[-k(R-r)]$, and

$$\omega^2 \simeq gk, \quad 2.16$$

which is independent of the stratification of the Sun.

In the atmosphere, $\omega_+ \simeq \omega_c$ for the values of k that have been observed (see Figure 2). Modes whose frequencies are comparable with this value have vertical wavelengths that are comparable with the scale of variation of ω_+ , and an accurate description of the oscillations requires a more careful treatment of the wave equation (2.2) than has been given here. Nevertheless, the condition $K^2 > 0$ provides a rough guide and indicates that a wave is trapped within the Sun only if its frequency is less than the value of ω_c characteristic of the atmosphere. This frequency corresponds to a period of about 3 min. Notice that the horizontal wavelengths of the modes are rather greater than the wavelengths in the vertical. Therefore, in a single oscillation period, information cannot be communicated over a distance great enough to recognize the horizontal variation of the wave, and the dynamics is locally independent of l . Consequently, the criterion for

propagation derived by Christensen-Dalsgaard et al. (24) for radial modes (using the more natural acoustical radius as the independent variable) and the subsequent discussions by Christensen-Dalsgaard & Frandsen (26, 28) are relevant to all the observed nonradial p modes.

Notice also that, in principle, modes such as the highest-frequency mode indicated in Figure 1 can be trapped between the two maxima of ω_+ in the chromosphere. These have been called chromospheric modes. Since the evanescent barriers between the zones of propagation are quite thin, significant penetration can occur, and the modes can have substantial amplitudes simultaneously in more than one zone. Gravity waves can also be trapped in the atmosphere.

Except when both n and l are small, the wave-induced perturbation Φ' to the gravitational potential is small and hardly influences the frequencies. Cowling (40) provided some justification for ignoring Φ' , even when l or n is not large, and to do so has subsequently become known as the Cowling approximation. It provides a good qualitative description of high-order monopole and dipole modes and of all modes with $l \geq 2$.

The resonant cavities are clearly defined only for modes of very high order or very high degree. Otherwise, the decline in amplitude through the evanescent regions is gentle, and modes can exist simultaneously in more than one cavity. As is evident in Figure 1, a mode can behave like a gravity wave in one part of a star and an acoustic wave in another. It is sometimes convenient to discuss oscillations in these terms (e.g. 155), but it is also useful to be able to assign a precise value to the order n without computing a large part of the spectrum of modes in order to apply the definition suggested in the Appendix. In the Cowling approximation, this is straightforward. Eckart (61) discusses how the phase differences between vertical displacement and pressure fluctuation decrease with height for p modes and increase for g modes, so that n can be computed by first assigning a sign to each zero in Ξ according to the direction of variation of the phase difference, and then counting the zeros algebraically. This criterion was first applied to stellar oscillations by Scuflaire (137) and Osaki (122). It has subsequently been found to work well for oscillations with $l \geq 2$ of most stars (including the Sun) when Φ' is correctly taken into account, though no wholly reliable simple criterion valid for low l has yet been found.

3. OBSERVATIONAL METHODS

The basic observations leading to the discovery of the resonant oscillations have all been carried out with conventional solar telescopes equipped with conventional spectrographs. The Doppler effect was used to determine the oscillatory velocities in selected spectral lines (64, 99, 115). Sometimes the

central intensity of a line has been used as an indicator of temperature fluctuations associated with the oscillations (117). The sensitivity of the Doppler measurement with this type of instrumentation, using photoelectric detectors, is typically about $10 \text{ ms}^{-1}/(5 \text{ arcsec})^2/\text{s}$. Recognition of the importance of measuring a substantial fraction of the solar surface has led to the development of various scanning techniques, either in one dimension, with a pointlike scanning aperture (44) or with a long rectangular aperture (128), or in two dimensions, using array detectors (16, 63).

One- or two-dimensional spatial resolution is necessary to distinguish the high-degree oscillation modes. The signal of low-degree modes has been extracted from observations with little or no spatial resolution, without scanning. Some observers have compared the Doppler shift in light from an outer annulus of the solar image with that from either the entire image (105) or a circular portion of it (50); others have worked with integrated light from the entire solar disk (14, 92). The differential method eliminates the velocity of the detector relative to the Sun and also much of the noise introduced by the spectrograph. It is most sensitive to modes of degree somewhat higher than those selected by the whole-disk measurements (33).

To obviate the instability of large spectrographs arising from internal seeing and the impracticality of an absolute wavelength reference, other groups of investigators have developed devices with high spectral resolution using resonance scattering of the sunlight by a suitable alkali vapor (14, 92). The comparatively low quantum efficiency of these detectors is unimportant if the instrument is used to analyze light integrated from much or all of the solar disk. A sensitivity of a fraction of 1 ms^{-1} per individual measurement is then achieved. Such high sensitivity is needed to detect the low-amplitude signals from individual modes of oscillation. The performance of a magneto-optical filter (20), which combines the high wavelength stability of resonant scattering devices with imaging capability, is presently being studied (125).

The new development of a "Fourier tachometer" (asymmetric Michelson interferometer placed behind a broadband prefilter in combination with panoramic detector arrays) takes advantage of high quantum efficiency to obtain stable measurements of the Doppler radial velocity with arbitrary spatial resolution (63).

An active cavity radiometer has recently been flown on the *Solar Maximum Mission* (SMM) to record temporal fluctuations of the solar luminosity (159). With its high stability (better than 10^{-6}), this instrument is capable of recording the extremely low-amplitude brightness oscillations of the integrated solar disk (160).

Observations of the solar limb have provided yet another means of

studying pulsations, either by measuring fluctuations of the apparent diameter of the solar disk (21) or by looking locally at changes of the structure of the limb-darkening function in the vicinity of its inflection point (12, 147, 163). H. Hill and his coworkers, who started this branch of helioseismology, have developed a sophisticated numerical procedure to overcome the tremendous difficulties imposed by the various seeing effects of the terrestrial atmosphere on the interpretation of these measurements (19, 98). Recently, another experiment for limb measurements has been put into operation, which relies both on the ability to “freeze” the solar image by rapid scanning and on an observing site with superior seeing (130).

4. HIGH-DEGREE MODES

In an extensive study of the five-minute oscillations using a spatio-temporal Fourier decomposition of Doppler and brightness data, Frazier (69) discovered that power was concentrated in two regions in the k - ω plane, one of which was situated where atmospheric waves are evanescent. This finding was already suggestive of normal modes trapped beneath the photosphere.

It took considerable further effort before the dispersion relation could be measured (44, 128). The observations were designed to isolate sectoral (and nearly sectoral) modes, which resemble plane waves propagating around a narrow equatorial zone. The characteristic parabolic dispersion relation (2.12) was evident for modes with $l \gtrsim 100$ (see Figure 2), and the close agreement of that relation with the eigenfrequencies of a solar model, already computed by Ulrich (151) at Frazier's instigation, convincingly established the nature of the oscillations: they are f modes and p modes of high degree. The oscillations are coherent in space and time over intervals at least as large as the limits attained by the observations (1000 Mm, 0.5 days). It has not been possible to resolve individual modes, so the power spectrum is a series of continuous ridges.

The detection and identification of these modes was soon followed by attempts to search for other high-degree modes. Chromospheric p modes with periods near 240 s and 180 s may have been detected by T. Duvall & J. Harvey (private communication) and Kneer et al. (104), and ridge structure in the k - ω diagram at frequencies below 1 mHz [Brown & Harrison (18)] is suggestive of g modes trapped in the atmosphere. In the last two studies, brightness fluctuations, rather than velocities, were observed. Because modes that are confined to the atmosphere have comparatively little inertia, they are prone to scattering by spatial and temporal atmospheric inhomogeneities. This exacerbates the observational problems resulting from seeing and instrumental noise.

Propagating acoustic waves generated, for example, by convective turbulence are expected in the atmosphere at frequencies above the cutoff frequency. By radiative and shock dissipation, and by coupling to MHD modes, they may contribute substantially to the heating of the lower chromosphere. Although these very high-degree oscillations have been

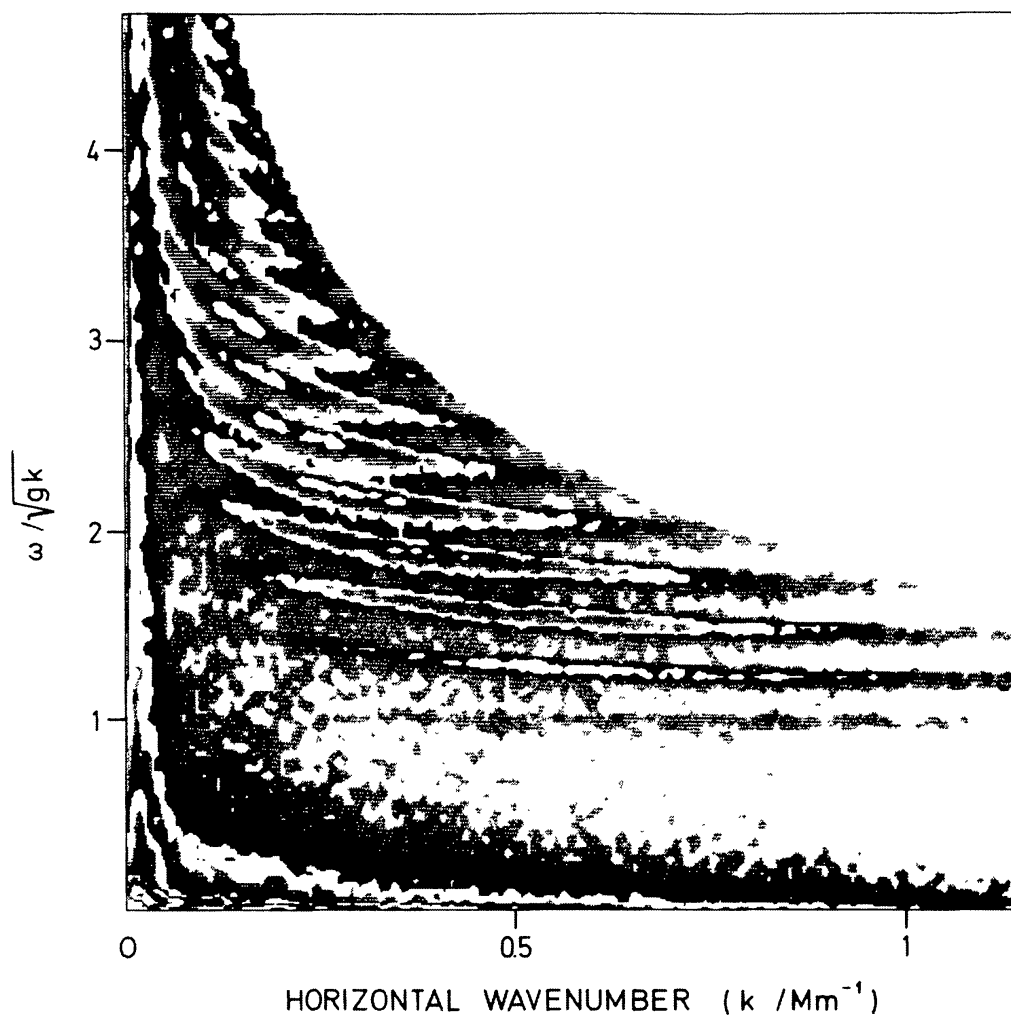


Figure 2 Two-dimensional power spectrum of high-degree five-minute oscillation data obtained by Deubner (47a). Different shadings signify different levels of power in the k - σ plane, where $\sigma = \omega/\sqrt{gk}$. The horizontal ridge of power at $\sigma = 1$ is produced by the f mode. The remaining ridges are produced by p modes. All modes in a ridge have a common order n , and n increases as σ increases at fixed k . At large horizontal wave numbers, σ depends only weakly on k , which indicates that near the surface the variation of sound speed with depth is similar to that of a polytrope. The rise in σ at low k arises partly from the fact that at greater depths c^2 increases more rapidly. There is also a geometrical contribution: Because the Sun is spherical, deeply penetrating waves travel a shorter distance than they would if the solar envelope were plane; they return to the surface more quickly and therefore resonate at a higher frequency than that given by Equation 2.14. The curvature of the ridges is greater at higher order, because at fixed k the depth of penetration is an increasing function of frequency.

studied intensively for many years (42, 88, 112, 116, 119, 120, 136), only recently has their wave character been established more firmly (48, 62, 146). Since they are mainly an atmospheric phenomenon, we do not discuss them further here. However, results obtained from these studies may well be useful for measuring the structure of the Sun's atmosphere, with implications concerning the outer boundary conditions that must be imposed on oscillations in the solar envelope.

Solar Structure

The first inference to have been drawn from the dispersion relation concerned the stratification of the convection zone. The frequencies observed were lower than the theoretical eigenvalues that had previously been computed (1, 151). According to Equation 2.14, this implies that the mean gradient G characterizing the upper layers of the convection zone was too large in the theoretical models. To reduce it would entail lowering the superadiabatic temperature gradient in the upper convective boundary layer, which in turn leads to a reduction of the specific entropy in the adiabatic part of the convection zone; trends in standard solar envelope computations suggested that such a reduction would imply an increase of the depth D of the convection zone and a higher opacity in the radiative interior (73). Numerical envelope computations by Ulrich & Rhodes (153) were consistent with this suggestion, and subsequent analyses of the sensitivity of the eigenfrequencies to other uncertain aspects of solar envelope models (8, 9, 118) seem to have ruled out other possibilities. Thus it appears that $D \simeq 2.0\text{--}2.3$ Mm. When coupled with the so-called standard stellar evolution theory, this value implies an initial solar helium abundance $Y_0 \simeq 0.25$.

More recently, Duvall (52) has pointed out that the observed dispersion relation is such that $(n + \epsilon)/\omega$ is a function of ω/k alone, where ϵ is constant. His results, together with more recent data from modes of low and intermediate degree obtained by Duvall & Harvey (53, 55), are displayed in Figure 3. This is the law for nondispersive waves in a waveguide of fixed dimensions, and it can be seen to follow from Equation 2.13, provided ω_c^2 does not contribute substantially to the integral. Of course, the dimensions of the solar waveguide are not fixed, but the law is preserved because the depth of penetration of the waves is also a function of ω/k . Gough (81) and Christensen-Dalsgaard et al. (24a) have discussed how Duvall's law can be used to estimate the variation of c with depth. The law also puts limits on the amount of local dispersion in the waves, and hence on the degree of contamination by buoyancy (81); it is the first explicit demonstration that the bulk of the convection zone is close to being adiabatically stratified.

Subphotospheric Velocities

Horizontal flow advects the wave pattern of high-degree five-minute modes at a speed equal to the mean flow speed, weighted by the energy density of the oscillation (74, 87). This shifts the ridge positions in the k - ω power spectrum. The original interest was in measuring the subphotospheric rotation, and early results of Deubner et al. (49) indicated that at some depth the velocity, which was presumed to indicate rotation, exceeded that at the photosphere (74). Subsequent observations by Rhodes et al. (126)

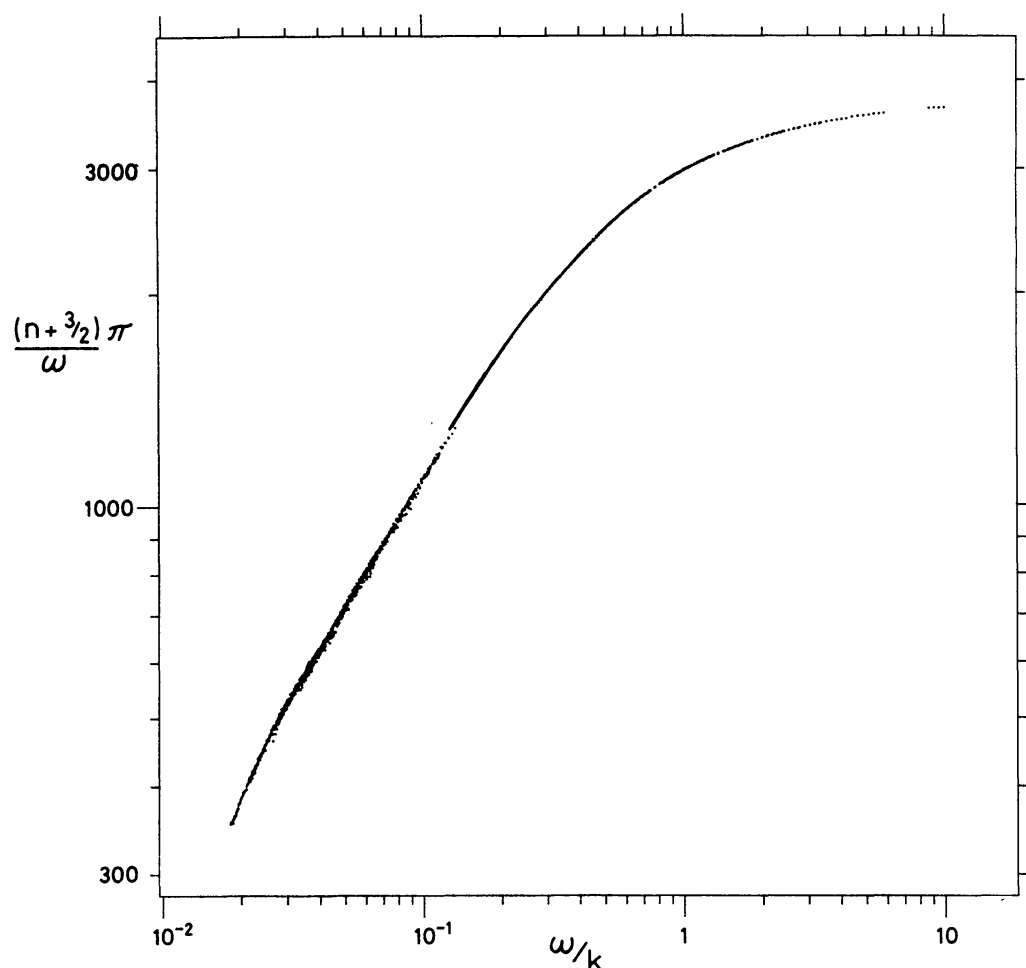


Figure 3 Representation, in the manner of Duvall (52), of 2783 five-minute modes of oscillation reported by Duvall (52) and Duvall & Harvey (53, 55), with degrees l ranging from 1 to 892 [from Christensen-Dalsgaard et al. (24a)]. Frequency ω is measured in s^{-1} , and the photospheric phase speed $v = \omega/k$ in units of Mm s^{-1} . It is evident from the discussion of resonant cavities, that the angular speed v/R of the wave pattern in the photosphere is approximately equal to the angular speed c/r of a sound wave propagating horizontally at the lower boundary $r = r_1$ of the region of propagation.

Subphotospheric Velocities

Horizontal flow advects the wave pattern of high-degree five-minute modes at a speed equal to the mean flow speed, weighted by the energy density of the oscillation (74, 87). This shifts the ridge positions in the k - ω power spectrum. The original interest was in measuring the subphotospheric rotation, and early results of Deubner et al. (49) indicated that at some depth the velocity, which was presumed to indicate rotation, exceeded that at the photosphere (74). Subsequent observations by Rhodes et al. (126)

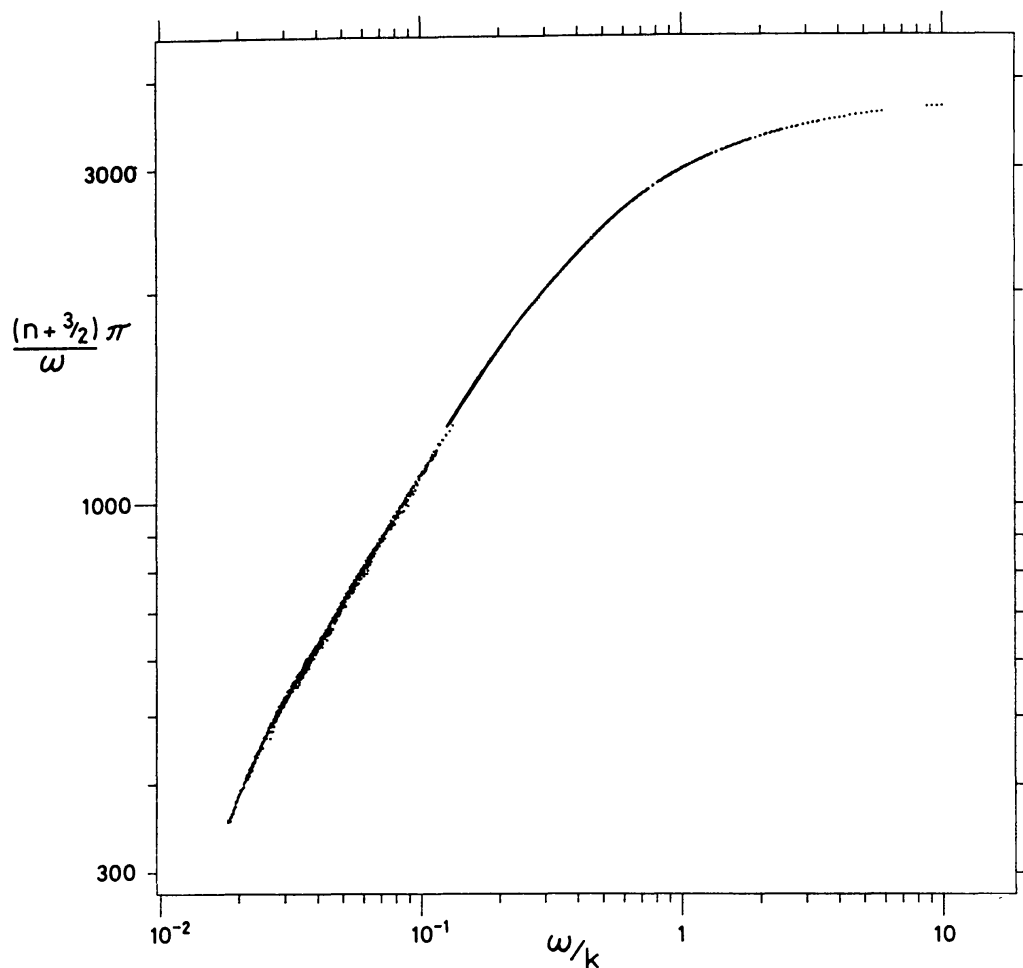


Figure 3 Representation, in the manner of Duvall (52), of 2783 five-minute modes of oscillation reported by Duvall (52) and Duvall & Harvey (53, 55), with degrees l ranging from 1 to 892 [from Christensen-Dalsgaard et al. (24a)]. Frequency ω is measured in s^{-1} , and the photospheric phase speed $v = \omega/k$ in units of Mm s^{-1} . It is evident from the discussion of resonant cavities, that the angular speed v/R of the wave pattern in the photosphere is approximately equal to the angular speed c/r of a sound wave propagating horizontally at the lower boundary $r = r_1$ of the region of propagation.

and apparently surpassed by the University of Birmingham group [Claverie et al. (38, 39)]. A power spectrum of the most recently analyzed data is shown in Figure 5. Pairs of modes with cyclic frequencies separated by $\delta_{n,l}/2\pi$ are clearly visible. The pairs have alternately odd and even degrees and are distributed uniformly with separation $\simeq \nu_0$.

On an expanded frequency scale, a similar spectrum of earlier data appeared to exhibit a splitting of the degeneracy with respect to the

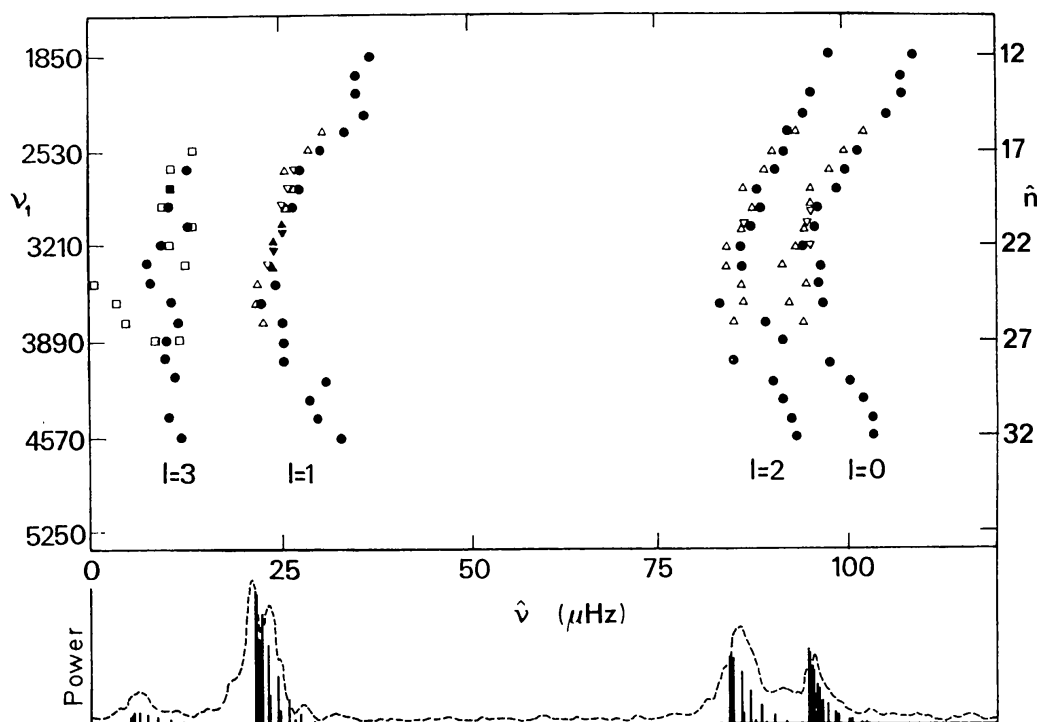


Figure 4 The upper portion is an echelle diagram of five-minute modes of low degree [after Scherrer et al. (134)]. A frequency axis is divided into 136- μ Hz segments, which are placed in a vertical row; a point in the resulting diagram represents the cyclic frequency ν of a mode according to $\nu = \nu_1 + \hat{\nu}$, where ν_1 and $\hat{\nu}$ are the ordinate and abscissa, respectively. The data have been compiled from various sources: ● Grec et al. (91), △ Claverie et al. (38), □ Scherrer et al. (135), ▽ Woodward & Hudson (160). Full symbols indicate coincidence (better than 0.5 μ Hz) with the South Pole data. The 136- μ Hz frequency interval is roughly the value of ν_0 defined by Equation 2.12. It follows from Equation 2.10 that the almost vertical columns correspond with modes of like degree l , with order n increasing downward in steps of unity. The values of l were inferred by comparing the superposed power spectrum of the observations (91), shown as a dashed curve in the lower part of the figure, with the theoretical predictions of power that are plotted as vertical lines in the manner of Christensen-Dalsgaard (23b). The amplitudes are computed as the product of the expectation of the actual amplitudes and the instrumental sensitivity (33). The orders of the modes are given by $n = \hat{n}$ for $l = 1, 2$ and $n = \hat{n} + 1, \hat{n} - 1$ for $l = 0$ and 3, respectively. The absolute values of \hat{n} were originally inferred from theory (30). They were subsequently confirmed unambiguously by the observations of Duvall & Harvey (53), which connected these data with the high-degree modes illustrated in Figure 2.

azimuthal order m : radial ($l = 0$) modes were unsplit, dipole ($l = 1$) modes appeared to be split into triplets, and there was evidence that quadrupole modes ($l = 2$) were split into quintuplets. The average splitting was $0.75 \mu\text{Hz}$, and this was interpreted as being produced by rotation. The observation is not what one would expect, however, because although there are $2l + 1$ values of m , modes with odd $l + m$ should not have been detected (33). Five-minute oscillations have also been found in the SMM-ACRIM intensity data (160, 161). The frequencies are in good agreement with those from Doppler measurements; however, it has not been possible to resolve degeneracy splitting (159a).

Whole-disk measurements of p modes are sensitive only to those modes with $l \lesssim 3$. Detection of five-minute modes with $l = 3, 4$, and 5 was achieved at Stanford University [Scherrer et al. (134, 135)] by subtracting Doppler signals from an inner disk and an outer annulus of the solar image. Octupole modes were identified by comparing frequencies with the South Pole and Birmingham data (see Figure 4), and the remaining values of l were deduced from theory. The results are in fair agreement with the whole-disk data, and they confirm the linear dependence of $\delta_{n,l}$ on $l(l + 1)$ at fixed $n + \frac{1}{2}l$ predicted by asymptotic theory.

VELOCITY POWER SPECTRUM

1981: 3 months. Tenerife&Hawaii, up to 22 hrs. per day

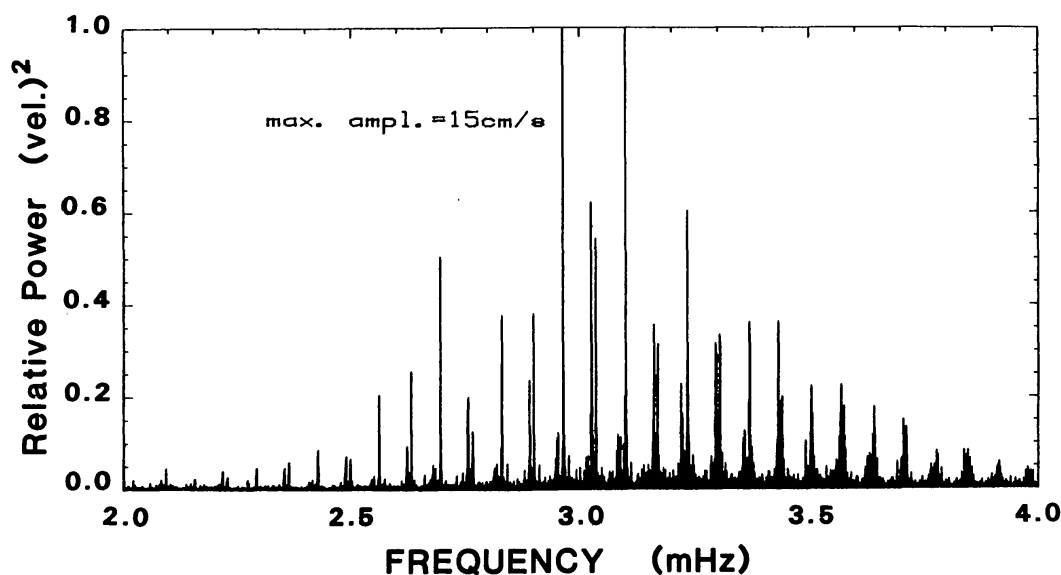


Figure 5 Power spectrum of combined whole-disk Doppler observations by the University of Birmingham group obtained from Hawaii and Tenerife over a period of 3 months. The separations $\delta_{n,l}$ between modes with like values of $n + \frac{1}{2}l$ are clearly visible.

Gravity Modes

Recently, evidence for low-degree g modes has been found in the Stanford (132) and Birmingham data (157), with periods of 3–5 hr, and in the SMM-ACRIM data (70), with periods of 4–140 hr. The method was to search among the highest peaks in the power spectra for sequences of frequencies corresponding to uniformly spaced periods, as is predicted by the asymptotic formulae (2.15) and (2.16). The high density of peaks (representing true eigenfrequencies, their aliases, and possibly noise) renders identification somewhat uncertain, and indeed the reports from Stanford and SMM, with $P_0 = 38.6$ min, conflict with the Birmingham data, from which it was inferred that $P_0 = 41.2$ min.

Solar Structure

The first diagnostic from low-degree modes to be discussed was the measure v_0 of the mean sound speed. Christensen-Dalsgaard & Gough (31) made a rough estimate of the mean separation between adjacent peaks in the p -mode power spectrum (of 36) and compared it with theoretical separations computed from a sequence of three solar models with different chemical composition. The separation observed was lower than expected. Within the confines of standard stellar evolution theory, the discrepancy suggested that the solar helium abundance might be somewhat low. A similar conclusion was subsequently drawn by Claverie et al. (36) using theoretical estimates extrapolated from the computations of Iben & Mahaffy (100). However, after refining the eigenfrequency computations and making a more detailed comparison between theory and observation, it became evident that precise agreement would not be possible (30); though the measured frequency separations in the 2–4 mHz range were lower than expected, the values of the frequencies themselves were rather high. In a sequence of solar models with varying initial helium abundance Y_0 , the frequency scale expands as Y_0 is increased, increasing both the values of the frequencies and their mean separation.

Subsequently, various workers have adjusted parameters in the theory, experimented with the equation of state, or added a mock magnetic field (70a, 121, 127, 138, 139, 140, 144, 152). They have been able to reduce the discrepancy, but they have not been able to remove it.

A diagnostic of considerable interest is the small separation $\Delta_{n,l} = \nu_{n,l} - \nu_{n-1,l+2}$; according to (2.10) and (2.11),

$$\Delta_{n,l} \simeq 2(2l+3)\alpha v_0^2 \nu_{n,l}^{-1}. \quad 5.1.$$

Noting the sensitivity of this expression to l , one would expect the region in the Sun that influences $\Delta_{n,l}$ to be contained sufficiently close to the center that sound can travel a horizontal wavelength in an oscillation period; for only there can a sound wave experience directly its horizontal variation.

Since $\omega_c \ll S_l$ in the core, it can be seen from Equations 2.6–2.8 that this condition is satisfied only in the region $r \lesssim r_1$. However, there the wave is evanescent. As r decreases below r_1 , the influence of the equilibrium state on the wave must diminish. Therefore, one might anticipate $\Delta_{n,l}$ to measure conditions close to r_1 .

Unfortunately, the situation is not quite that simple. First, since sound speed, and consequently the wavelength of the modes, is greater near the center, it is more difficult for p modes to resolve small-scale structure as r decreases. Second, it appears that terms in the asymptotic expansion of ω beyond those given in (2.10–2.12), and which include perturbations in the gravitational potential, might have a significant influence (W. Dziembowski & D. Gough, unpublished), so that oscillatory motion in the core is coupled instantaneously to the rest of the star. Nevertheless, the local contribution to $\Delta_{n,l}$ is probably the more important; it depends on the variation of c in the core, and decreases as the chemical inhomogeneity produced by nuclear reactions increases (82).

Theoretical computations by various groups (31, 144, 154) have been compared with the observations of Claverie et al. (38) and Fossat et al. (68) by Gough (79). The difference $\Delta_{n,l}$ varies slowly with n over the 2–4 mHz frequency range ($15 \lesssim n \lesssim 30$); its average, according to the observations, is about 9 and 15 μHz for $l = 0$ and 1, respectively. Standard unmixed solar models require an initial helium abundance Y_0 as great as 0.25 to produce such low values. These models have high neutrino fluxes. They also have relatively deep convection zones, in accord with the implications of the high-degree modes. Any partial mixing in the core is likely to increase $\Delta_{n,l}$ and consequently Y_0 would have to be increased to compensate.

Attempts to estimate Y_0 have been made by fitting by least-squares interpolated p -mode eigenfrequencies of a sequence of solar models to the observed five-minute frequencies. The procedure also determines the order n of the modes. By weighting all frequencies equally, Christensen-Dalsgaard & Gough (32) and Shibahashi et al. (144a) found $Y_0 = 0.27$ and 0.23, respectively. The best-fitting model does not agree with the g -mode data: The periods of g modes of that model corresponding to those reported by Scherrer & Delache (132), when fitted to Equation 2.15, yield $P_0 \approx 34.5$ min (83). To increase this value would require a reduction in the buoyancy frequency. This can be achieved either by mixing the interior (10, 10a) or by reducing Y_0 . Either would increase $\Delta_{n,l}$.

6. FIVE-MINUTE MODES OF INTERMEDIATE DEGREE

By projecting Doppler data onto zonal harmonics, Duvall & Harvey (53) have identified five-minute modes with $l \leq 140$, distinguishing more than

20 branches of the dispersion relation. Thus they were able to connect the previously acquired low-degree data with the high-degree modes and confirm the values of n that had already been inferred for the low-degree modes by model fitting (30, 32, 144a). These data satisfy the waveguide law (see Figure 3) found by Duvall (53) for high-degree modes. They also share with the low-degree modes the property that the ratio $(v_{n+1,l} - v_{n,l}) : v_{n,l}$ is lower than can be explained by theory. More recent attempts to isolate sectoral harmonics (54) have produced similar results.

A thorough comparison of intermediate-degree data with theory has not yet been made. However, preliminary analyses (34, 55) have revealed that the systematic discrepancy mentioned earlier between theoretical low-degree five-minute eigenfrequencies and observation has a frequency dependence that is independent of l for $l \lesssim 30$; at higher values of l , the dependence of the discrepancy on frequency changes. Recalling that the wave senses l directly only in the vicinity of its lower turning point at $r = r_1$ leads one to conclude that the most deep-seated error in the theoretical model that has a substantial influence on p modes is likely to be located somewhere near the level at which $S_{30} \simeq \omega$. This is near the base of the convection zone.

There are several other programs to measure modes of intermediate degree. Spatial resolution is to be achieved either by sequential scanning of the solar image (15) or by arrays of detectors (53, 63). Groups of modes can be isolated by performing suitable projections of the data (23c). Individual modes cannot be isolated at any one instant, because for this it would be necessary to view the entire surface of the Sun, but there are grounds to anticipate that a subsequent comparison of the temporal information with theory could separate the individual modes in each group (17).

7. LIMB OBSERVATIONS

At about the same time as the first measurement of the dispersion relation for high-degree modes (44) and the discovery of discrete frequencies in spatially unresolved observations (13, 141), H. Hill and his collaborators (97) reported an accidental detection of oscillations in the apparent diameter of the Sun. There followed a considerable dispute over whether or not the origin of these oscillations is solar (e.g. 67, 95). Many of the objections, which related to atmospheric distortions of the solar image, have been circumvented in the most recent observations (12, 130), where local fluctuations in the limb-darkening function were analyzed. Nevertheless, the interpretation of even these data is still in doubt.

Current limb observations are most sensitive to oscillations of degree $l \lesssim 50$ (94). They do not have the spatial and temporal resolution to separate the individual modes, except possibly for frequencies roughly in

the range 0.4–0.6 mHz, where the higher-degree modes do not exist. There is reasonable hope (85), however, that with more spatial information, future limb observations might provide valuable information about the modes of low order.

8. PROBLEMS FOR THE IMMEDIATE FUTURE

Our discussion has been concerned mainly with the hydrostatic stratification of the Sun, for this is the aspect of the solar structure about which oscillations have so far yielded the most reliable information. However, it is already apparent that this is merely the first step in a subject that promises to progress significantly in the next decade. There are good reasons to believe that we shall soon put useful bounds on large-scale asymmetries in the structure of the Sun that split the degeneracy with respect to m in the oscillation eigenfrequencies. These will no doubt raise new questions about the internal dynamics of the Sun.

Asid  from improvements in our knowledge of the density stratification, an issue with which we are most likely to make imminent progress is the distribution of angular momentum within the Sun. This has an obvious direct bearing on the internal dynamics of stellar spin-down and is likely to shed light on ill-understood questions of wave transport. The ramifications concern material mixing by Ekman-Eddington-Sweet circulation and the influence of the centrifugally induced distortion of the gravitational potential on the precession of planetary orbits (20a, 55a, 77, 96).

Several reports of rotational splitting have been made (39, 43, 54, 96). Taken at face value they all imply that somewhere at depth, rotation is more rapid than at the surface, though by how much is not yet clear. Unless one accepts that the Sun's angular velocity Ω is a rapidly varying function of position or time, the data appear to be contradictory (81). The most extensive data (54) suggest that throughout most of the Sun, Ω is somewhat less than the equatorial angular velocity in the photosphere, and that in a central core (corresponding roughly to where nuclear reactions have raised the molecular weight) Ω is substantially greater than it is elsewhere (55a).

Degeneracy splitting by intense magnetic fields might also enrich the spectrum (49a, 58, 59, 78, 86).

Recent developments in instrumentation for making spatially resolved observations (e.g. 63) will no doubt permit us to improve substantially our measurements of high-degree modes. Thus, we might make coarse measurements of velocity and temperature variations immediately beneath the photosphere, although the extent to which they will be able to resolve any of the theoretical issues about the dynamics of the convection zone is still an open question. There is perhaps more hope for high temporal resolution of modes of low degree. Here, one is hindered less by the problems of seeing

through the Earth's atmosphere. Variations in the eigenfrequencies of these modes during the course of the solar cycle are likely to be large enough to be detectable (80), and they may reveal whether the cycle is controlled by a turbulent dynamo in the convection zone or by some more deep-seated process.

It may be necessary to restrict attention to modes of relatively low order, because the lifetimes of the high-order oscillations may be insufficient for accurate eigenfrequencies to be determined. Short lifetimes of high-frequency modes were predicted by theory (71, 75), and now there is also evidence from the observations: The peaks in Figure 5 are substantially broader at high frequencies. It is also evident from Figure 5 that the amplitudes of the lowest-order modes are small, rendering it difficult to extract the signal of the regular oscillations from the background noise.

Almost all the diagnostic studies that have been made have relied on model fitting. Oscillation eigenfrequencies of a solar model defined by certain parameters are computed (this is called the "forward problem"), and the parameters are adjusted to find the model that best fits the observations. This procedure has the advantage of being relatively simple. It also provides useful insight, especially if the parameters have a clear physical significance. However, inverse calculations designed to extract certain aspects of the structure of the Sun directly from the data are likely to increase substantially our diagnostic capabilities. A variety of methods apparently suitable for helioseismology have been developed by geophysicists (6, 7, 103, 123, 124, 131, 158) and used with considerable success to infer the structure of the Earth. The product of the techniques is a theoretical model, together with an estimate of its accuracy. A few inverse calculations have been performed on artificial solar data (34, 74, 83, 84) to assess what information is likely to be acquired from future observations.

Any diagnostic calculation depends on knowing in considerable detail the physics of the oscillations. In the Sun there are many uncertainties, so our problems are exacerbated. In particular, the equation of state is inadequately understood, so we could not calculate the sound speed accurately even if we knew the composition and thermodynamic state of the gas (129). Of course, there may be sufficient information in the oscillation eigenfrequencies to impose important constraints on the possible forms of the equation of state in the dense interior (81), adding yet another role to the Sun as a physics laboratory.

It is not only an analysis of oscillation eigenfrequencies that is likely to provide valuable information about the solar interior. The principal processes that excite waves and control their amplitudes are also important. At present we do not know what these are. Some have maintained that the oscillations are self-excited by modulating the thermal energy flow with an Eddington valve, in much the same way as in the Cepheids and RR Lyrae stars (2–5). In that case amplitudes might be limited by nonlinear coupling

to stable modes of oscillation (56, 57), but it is not yet clear whether this process can extract energy fast enough at the low amplitudes observed. Alternatively, the modes might be stable, as a result of their interaction with convection (9, 71). Stochastic fluctuations in the turbulence might then be responsible for forcing the modes to oscillate at low amplitude (72). Amplitude estimates based on this idea are roughly correct for solar five-minute oscillations (75), but other modes may need to be driven differently. What is required now is a careful assessment of all the nonlinear processes affecting the modes, perhaps along the lines proposed by Dolez et al. (51). If successful, it may then be possible to invert the argument to learn about convection.

Spatially unresolved oscillation measurements can be carried out on other stars. Christensen-Dalsgaard & Frandsen (27) have estimated amplitudes under the assumption that the modes are excited stochastically by turbulence, and they have concluded that on the main sequence, F stars are the most suitable candidates for study. As a result, Fossat (66) recently observed α Centauri and reported having detected oscillations. Also, Kurtz (108) appears to have found a rapidly oscillating Ap star to have a spectrum of p modes excited (143), like the Sun. These promising beginnings are likely to stimulate further interest in asteroseismology.

We cannot end this review without mentioning the 160-min oscillation. At first there was considerable doubt about its origin, particularly because its period is one ninth of a terrestrial day (89, 162). But now it seems likely that the oscillation is solar (106, 107, 133). However, its nature is still a mystery. The first plausible suggestion was that it is a low-degree g mode (29), but this then raised the question of why only one of a rich spectrum of modes should predominate. One possibility is that it is excited by a chance resonance between p modes (29, 73). If so, the potential modification of the accuracy of the resonance during the solar cycle might have interesting observable consequences. Isaak (102) has suggested that the oscillation is driven by the gravitational radiation from a close binary star. On the other hand, Childress & Spiegel (22) have argued that the oscillation may not be a linear mode at all, but instead is caused by a soliton propagating around the solar core and driven by the perturbations it produces in the nuclear reactions. More exotic but unproven suggestions have been entertained (11).

After the five-minute modes, this long-period oscillation was the first to be discovered. It may be the last to be explained.

ACKNOWLEDGMENTS

We are grateful to G. Isaak and his colleagues for providing us with Figure 5, and to J. Christensen-Dalsgaard both for his help in producing Figure 1 and for his comments on the original manuscript.

APPENDIX

CLASSIFICATION OF STELLAR OSCILLATIONS It is important to define a precise nomenclature in order to avoid ambiguity. Since to a first approximation the equilibrium state of the Sun is spherically symmetrical, linearized vertical displacements can be represented as a superposition of normal modes of the form (2.1). The vertical velocity and the perturbations in all thermodynamical state variables have a similar form.

Under certain idealized conditions (e.g. adiabatic motion and perfect reflection of the waves at the stellar surface), the governing equations of motion and their boundary conditions admit a sequence of discrete eigensolutions for which Ξ and ω are real. These can be arranged in order of increasing ω . The modes are then labeled sequentially with an integer n , which is called the *order* of the mode. In reality the idealized conditions are not met precisely, though they are a good approximation in the Sun for the modes that have been observed. Therefore, the true modes are quite similar to the idealized ones, and n is probably well defined.

There has been some diversity in the naming of l and m ; here, we call the degree l of the associated Legendre function the *degree* of the mode, and the order m we call the *azimuthal order* of the mode.

Formally, the frequency is unbounded below (except when $l = 0$), and were it not for the solar atmosphere it would also be unbounded above (see Section 2). Therefore it is not immediately obvious where to choose the origin of n , and again there is some diversity in the literature. It appears to be possible (though it has not yet been proved) to choose n such that as $n \rightarrow \pm \infty$ at fixed l , $|n|$ is the number of zeros in Ξ (excluding the zero at $r = 0$ when $l \geq 2$). In the case of the spherically symmetrical modes ($l = 0$), we label the lowest-frequency (or fundamental) mode with $n = 1$; once again n is the number of zeros in Ξ when n is large, although now the zero at $r = 0$ must be counted.

In simple stellar models, modes with $n > 0$ and $n < 0$ have the characteristics of acoustic and internal gravity waves; they were designated p modes and g modes by Cowling (40). Modes with $n = 0$ are essentially surface gravity waves. They are the fundamental g modes, or f modes, and have the property that when $l \gg 1$ they have no zeros in Ξ .

In this review we have adopted the common practice of ignoring the sign of n and designating the mode with g , f , or p . Then both the g and p sequences start from $n = 1$. A p mode with $n = 2$ and $l = 3$, for example, is designated $p_2(l = 3)$. Spherically symmetric gravity modes cannot exist, so the $l = 0$ modes are p modes. This is partly why the fundamental $l = 0$ mode was labeled with $n = 1$. There is also a mathematical reason for this choice, but we do not discuss that here.

In the case of high-degree g modes, such as the lowest-frequency mode

illustrated in Figure 1, the decline in amplitude in the evanescent region immediately beneath the photosphere is very severe (25, 60), and communication between the two regions of propagation is extremely small. Except in cases of accurate resonance between oscillations trapped in the two regions of propagation (which is a mathematical possibility for essentially undamped oscillation modes of idealized solar models, but is unlikely to be relevant in practice), the interior and the atmosphere oscillate independently. Consequently, it is sometimes expedient to classify the interior and atmospheric modes separately (155). Otherwise, a modification to the structure of the atmosphere that has no influence on the interior could change the formal classification of a mode that exists essentially only beneath the convection zone. Notice that in this scheme a theoretical mode that happens to resonate with both the interior and the atmosphere would be classified twice.

In reality, stars are not spherically symmetrical, for they rotate and contain magnetic fields. The oscillation eigenfunctions are no longer precisely of the form (2.1), and, in particular, the degeneracy of the frequency with respect to m is split. Nevertheless, in the Sun the deviations from spherical symmetry are small, and except in certain rare cases of resonance (which we do not discuss here), the modifications to the normal modes are small too. Thus we can identify without ambiguity the corresponding modes of a similar spherically symmetrical model of the Sun, and we adopt the classification of the latter for the solar modes.

Literature Cited^a

1. Ando, H., Osaki, Y. 1976. *Publ. Astron. Soc. Jpn.* 27: 581–603
2. Ando, H., Osaki, Y. 1977. *Publ. Astron. Soc. Jpn.* 29: 221–33
3. Antia, H. M., Chitre, S. M. 1984. In CATANIA. In press
4. Antia, H. M., Chitre, S. M., Kale, D. M. 1978. *Sol. Phys.* 56: 275–92
5. Antia, H. M., Chitre, S. M., Narasimha, D. 1982. *Sol. Phys.* 77: 303–27
6. Backus, G. E., Gilbert, J. F. 1967. *Geophys. J. R. Astron. Soc.* 13: 247–76
7. Backus, G. E., Gilbert, J. F. 1970. *Philos. Trans. R. Soc. London Ser. A* 266: 123–92
8. Belvedere, G., Gough, D. O., Paternò, L. 1983. *Sol. Phys.* 82: 343–54
9. Berthomieu, G., Cooper, A. J., Gough, D. O., Osaki, Y., Provost, J., Rocca, A. 1980. In TUCSON, pp. 307–12
10. Berthomieu, G., Provost, J., Schatzman, E. 1984. In CATANIA. In press
- 10a. Berthomieu, G., Provost, J., Schatzman, E. 1984. *Nature* 308: 254–57
11. Blinnikov, S. I., Khlopov, M. Yu. 1983. *Sol. Phys.* 82: 383–85
12. Bos, R. J., Hill, H. A. 1983. *Sol. Phys.* 82: 89–102
13. Brookes, J. R., Isaak, G. R., van der Raay, H. B. 1976. *Nature* 259: 92–95
14. Brookes, J. R., Isaak, G. R., van der Raay, H. B. 1978. *MNRAS* 185: 1–17
15. Brookes, J. R., Isaak, G. R., van der Raay, H. B. 1981. *Sol. Phys.* 74: 503–8

^a We use the following abbreviated notations for some frequently cited conference proceedings:

TUCSON = *Nonradial and Nonlinear Stellar Pulsation*, ed. H. A. Hill, W. A. Dziembowski. Berlin: Springer. 497 pp.
 CATANIA = *Oscillations as a Probe of the Sun's Interior*, ed. G. Belvedere, L. Paterno. *Mem. Soc. Astron. Ital.* In press
 SNOWMASS = *Solar Seismology from Space*, ed. J. W. Harvey, E. J. Rhodes, Jr., J. Toomre, R. K. Ulrich. Washington DC: NASA. In press

16. Brown, T. M. 1981. In *Solar Instrumentation: What's Next?*, ed. R. B. Dunn, pp. 150–54. Sunspot, N. Mex.: Sacramento Peak Obs.
17. Brown, T. M., Christensen-Dalsgaard, J., Mihalas, B. 1984. In SNOWMASS. In press
18. Brown, T. M., Harrison, R. L. 1980. *Ap. J. Lett.* 236: L169–73
19. Brown, T. M., Stebbins, R. T., Hill, H. A. 1978. *Ap. J.* 223: 324–38
20. Cacciani, A., Rhodes, E. J. Jr., Ulrich, R. K., Howard, R. 1984. In SNOWMASS. In press
- 20a. Campbell, L., McDow, J. C., Moffat, J. W., Vincent, D. 1983. *Nature* 305: 508–10
21. Caudell, T. P., Knapp, J., Hill, H. A., Logan, J. D. 1980. In TUCSON, pp. 206–18
22. Childress, S., Spiegel, E. A. 1981. In *Variations of the Solar Constant*, ed. S. Sofia, pp. 273–91. *NASA Conf. Publ.* 2191
23. Christensen-Dalsgaard, J. 1980. *MNRAS* 190: 765–91
- 23a. Christensen-Dalsgaard, J. 1982. *MNRAS* 199: 735–61
- 23b. Christensen-Dalsgaard, J. 1983. *Adv. Space Res.* 2: 11
- 23c. Christensen-Dalsgaard, J. 1984. In SNOWMASS. In press
24. Christensen-Dalsgaard, J., Cooper, A. J., Gough, D. O. 1983. *MNRAS* 203: 165–79
- 24a. Christensen-Dalsgaard, J., Duvall, T. L. Jr., Gough, D. O., Harvey, J. W. 1984. *Nature*. In press
25. Christensen-Dalsgaard, J., Dziembowski, W., Gough, D. O. 1980. In TUCSON, pp. 313–41
26. Christensen-Dalsgaard, J., Frandsen, S. 1983. *Sol. Phys.* 82: 165–204
27. Christensen-Dalsgaard, J., Frandsen, S. 1983. *Sol. Phys.* 82: 469–86
28. Christensen-Dalsgaard, J., Frandsen, S. 1984. In CATANIA. In press
29. Christensen-Dalsgaard, J., Gough, D. O. 1976. *Nature* 259: 89–92
30. Christensen-Dalsgaard, J., Gough, D. O. 1980. *Nature* 288: 544–47
31. Christensen-Dalsgaard, J., Gough, D. O. 1980. In TUCSON, pp. 184–90
32. Christensen-Dalsgaard, J., Gough, D. O. 1981. *Astron. Astrophys.* 104: 173–76
33. Christensen-Dalsgaard, J., Gough, D. O. 1982. *MNRAS* 198: 141–71
34. Christensen-Dalsgaard, J., Gough, D. O. 1984. In SNOWMASS. In press
35. Deleted in proof
36. Claverie, A., Isaak, G. R., McLeod, C. P., van der Raay, H. B., Roca Cortez, T. 1979. *Nature* 282: 591–94
37. Claverie, A., Isaak, G. R., McLeod, C. P., van der Raay, H. B., Roca Cortez, T. 1980. *Astron. Astrophys. Lett.* 91: L9–10
38. Claverie, A., Isaak, G. R., McLeod, C. P., van der Raay, H. B., Roca Cortez, T. 1981. *Nature* 293: 443–45
39. Claverie, A., Isaak, G. R., McLeod, C. P., van der Raay, H. B., Roca Cortez, T. 1982. *Sol. Phys.* 74: 51–57
40. Cowling, T. G. 1941. *MNRAS* 101: 367–75
41. Cox, J. P. 1980. *Theory of Stellar Pulsation*. Princeton Univ. Press. 380 pp.
42. Cram, L. E. 1978. *Astron. Astrophys.* 70: 345–54
43. Delache, P., Scherrer, P. H. 1983. *Nature* 306: 651–53
44. Deubner, F.-L. 1975. *Astron. Astrophys.* 44: 371–75
45. Deubner, F.-L. 1976. In *The Energy Balance and Hydrodynamics of the Solar Chromosphere and Corona*, ed. R. M. Bonnet, P. Delache, pp. 45–68. Clairmont-Ferrand: G. de Bussac
46. Deubner, F.-L. 1980. In *Highlights of Astronomy*, ed. P. A. Wayman, 5: 75–87. Dordrecht: Reidel
47. Deubner, F.-L. 1981. In *The Sun as a Star*, ed. S. Jordan, pp. 65–84. *NASA-SP-450*
- 47a. Deubner, F.-L. 1983. *Sol. Phys.* 82: 103–9
48. Deubner, F.-L., Endler, F., Staiger, J. 1984. In CATANIA. In press
49. Deubner, F.-L., Ulrich, R. K., Rhodes, E. J. Jr. 1979. *Astron. Astrophys.* 72: 177–85
- 49a. Dicke, R. H. 1982. *Nature* 300: 693–97
50. Dittmer, P. H. 1977. PhD thesis. Stanford Univ., Stanford, Calif.
51. Dolez, N., Poyet, J.-P., Legait, A. 1984. In CATANIA. In press
52. Duvall, T. L. Jr. 1982. *Nature* 300: 242–43
53. Duvall, T. L. Jr., Harvey, J. W. 1983. *Nature* 302: 24–27
54. Duvall, T. L. Jr., Harvey, J. W. 1984. *Nature*. In press
55. Duvall, T. L. Jr., Harvey, J. W. 1984. In SNOWMASS. In press
- 55a. Duvall, T. L. Jr., Dziembowski, W. A., Goode, P. R., Gough, D. O., Harvey, J. W., Leibacher, J. W. 1984. *Nature*. In press
56. Dziembowski, W. A. 1982. *Acta Astron.* 32: 147–71
57. Dziembowski, W. A. 1983. *Sol. Phys.* 82: 259–66
58. Dziembowski, W. A., Goode, P. R. 1983. *Nature* 305: 39–42
59. Dziembowski, W. A., Goode, P. R. 1984. In CATANIA. In press

60. Dziembowski, W. A., Pamjatnykh, A. A. 1978. In *Pleins Feux sur la Physique Solaire*, ed. J. Rösch, pp. 135–40. Paris: CNRS
61. Eckart, C. 1960. *Hydrodynamics of Oceans and Atmospheres*. London: Pergamon
62. Endler, F., Deubner, F.-L. 1983. *Astron. Astrophys.* 121: 291–96
63. Evans, J. W. 1981. In *Solar Instrumentation: What's Next?*, ed. R. B. Dunn, pp. 150–54. Sunspot, N. Mex: Sacramento Peak Obs.
64. Evans, J. W., Michard, R. 1962. *Ap. J.* 135: 812–21
65. Evans, J. W., Michard, R. 1962. *Ap. J.* 136: 493–506
66. Fossat, E. 1984. In CATANIA. In press
67. Fossat, E., Grec, G., Harvey, J. W. 1981. *Astron. Astrophys.* 94: 95–99
68. Fossat, E., Grec, G., Pomerantz, M. 1981. *Sol. Phys.* 74: 59–63
69. Frazier, E. N. 1968. *Z. Ap.* 68: 345–56
70. Fröhlich, C., Delache, P. 1984. In CATANIA. In press
- 70a. Gabriel, G., Scuflaire, R., Noels, A. 1982. *Astron. Astrophys.* 110: 50–53
- 70b. Gingerich, O., Noyes, R. W., Kalkofen, W., Cuny, Y. 1971. *Sol. Phys.* 18: 347–65
71. Goldreich, P., Keeley, D. A. 1977. *Ap. J.* 211: 934–42
72. Goldreich, P., Keeley, D. A. 1977. *Ap. J.* 212: 243–51
73. Gough, D. O. 1976. In *The Energy Balance and Hydrodynamics of the Solar Chromosphere and Corona*, ed. R. M. Bonnet, P. Delache, pp. 3–36. Clairmont-Ferrand: G. de Bussac
74. Gough, D. O. 1978. *Proc. EPS Workshop Sol. Rotation*, ed. G. Belvedere, L. Paternò, pp. 255–68. Catania: Catania Univ. Press
75. Gough, D. O. 1980. In TUCSON, pp. 273–99
76. Gough, D. O. 1982. *Irish Astron. J.* 15: 118–19
77. Gough, D. O. 1982. *Nature* 298: 334–39
78. Gough, D. O. 1982. *Nature* 298: 350–54
79. Gough, D. O. 1983. *Proc. ESO Workshop Primordial Helium*, ed. P. A. Shaver, D. Kunth, K. Kjar, pp. 117–36. Garching: ESO
80. Gough, D. O. 1983. In *Pulsations in Classical and Cataclysmic Variables*, ed. J. P. Cox, C. J. Hansen, pp. 117–37. Boulder, Colo: JILA
81. Gough, D. O. 1984. In CATANIA. In press
82. Gough, D. O. 1983. *Phys. Bull.* 34: 502–7
83. Gough, D. O. 1984. In SNOWMASS. In press
84. Gough, D. O. 1984. *Philos. Trans. R. Soc. London Ser. A*. In press
85. Gough, D. O., Latour, J. 1984. *Astr. Expr.* 1: 9–25
86. Gough, D. O., Taylor, P. P. 1984. In CATANIA. In press
87. Gough, D. O., Toomre, J. 1983. *Sol. Phys.* 82: 401–10
88. Gouttebroze, P., Leibacher, J. W. 1980. *Ap. J.* 238: 1134–51
89. Grec, G., Fossat, E. 1979. *Astron. Astrophys.* 77: 351–53
90. Grec, G., Fossat, E., Pomerantz, M. 1980. *Nature* 288: 541–44
91. Grec, G., Fossat, E., Pomerantz, M. A. 1983. *Sol. Phys.* 82: 55–66
92. Grec, G., Fossat, E., Vernin, J. 1976. *Astron. Astrophys.* 50: 221–25
93. Hill, F., Toomre, J., November, L. J. 1983. *Sol. Phys.* 82: 411–25
- 93a. Hill, F., Gough, D. O., Toomre, J. 1984. In CATANIA. In press
94. Hill, H. A. 1978. In *The New Solar Physics*, ed. J. A. Eddy, pp. 135–214. Boulder, Colo: Westview
95. Hill, H. A., Bos, R. J., Caudell, T. P. 1983. *Sol. Phys.* 82: 129–38
96. Hill, H. A., Bos, R. J., Goode, P. R. 1982. *Phys. Rev. Lett.* 49: 1794–97
97. Hill, H. A., Stebbins, R. T., Brown, T. M. 1976. In *Atomic Masses and Fundamental Constants*, ed. J. H. Sanders, A. H. Wapstra, pp. 622–28. New York: Plenum
98. Hill, H. A., Stebbins, R. T., Oleson, J. R. 1975. *Ap. J.* 200: 484–98
99. Howard, R. 1967. *Sol. Phys.* 2: 3–33
100. Iben, I. Jr., Mahaffy, J. 1976. *Ap. J. Lett.* 209: L39–43
101. Isaak, G. R. 1982. *Nature* 296: 130–31
102. Isaak, G. R. 1984. In CATANIA. In press
103. Jackson, D. D. 1972. *Geophys. J. R. Astron. Soc.* 28: 97–109
104. Kneer, F., Newkirk, G. Jr., von Uexküll, M. 1982. *Astron. Astrophys.* 113: 129–34
105. Kotov, V. A., Severny, A. B., Tsap, T. T. 1978. *MNRAS* 183: 61–87
106. Kotov, V. A., Severny, A. B., Tsap, T. T., Moiseev, I. G., Efanov, V. A., Nesterov, N. S. 1983. *Sol. Phys.* 82: 9–19
107. Koutchmy, S., Koutchmy, O., Kotov, V. A. 1980. *Astron. Astrophys.* 90: 372–76
108. Kurtz, D. 1983. *MNRAS* 205: 11–22
109. Lamb, H. 1908. *Proc. London Math. Soc.* 7: 122–41
110. Lamb, H. 1932. *Hydrodynamics*. Univ. Cambridge Press. 6th ed.
111. Ledoux, P., Perdang, J. 1980. *Bull. Soc. Math. Belg.* 32: 133–59
112. Leibacher, J. W., Gouttebroze, P., Stein, R. F. 1982. *Ap. J.* 258: 393–403
113. Leibacher, J. W., Stein, R. F. 1971. *Astrophys. Lett.* 7: 191–92

114. Leibacher, J. W., Stein, R. F. 1981. In *The Sun as a Star*, ed. S. Jordan, pp. 263–88. *NASA SP-450*
115. Leighton, R. B. 1960. *Proc. IAU Symp.* 12: 321–25
- 115a. Leighton, R. B., Noyes, R. W., Simon, G. W. 1962. *Ap. J.* 135: 474–99
116. Lites, B. W., Chipman, E. G. 1979. *Ap. J.* 231: 570–88
117. Livingston, W., Milkey, R., Slaughter, C. 1977. *Ap. J.* 211: 281–87
118. Lubow, S. H., Rhodes, E. J. Jr., Ulrich, R. K. 1980. In *TUCSON*, pp. 300–6
119. Mein, N. 1977. *Sol. Phys.* 52: 283–92
120. Mein, N., Schmieder, B. 1981. *Astron. Astrophys.* 97: 310–16
121. Noels, A., Scuflaire, R., Gabriel, M. 1984. *Astron. Astrophys.* 130: 389–96
122. Osaki, Y. 1975. *Publ. Astron. Soc. Jpn.* 27: 237–58
123. Parker, R. L. 1977. *Ann. Rev. Earth Planet. Sci.* 5: 35–65
124. Parker, R. L. 1977. *Rev. Geophys. Space Phys.* 15: 446–56
125. Rhodes, E. J. Jr., Cacciani, A., Blamont, J., Tomczyk, S. 1984. In *SNOWMASS*. In press
126. Rhodes, E. J. Jr., Harvey, J. W., Duvall, T. L. Jr. 1983. *Sol. Phys.* 82: 111
127. Rhodes, E. J. Jr., Ulrich, R. K., Brunish, W. M. 1984. In *CATANIA*. In press
128. Rhodes, E. J. Jr., Ulrich, R. K., Simon, G. W. 1977. *Ap. J.* 218: 521–29
129. Rogers, F. 1984. In *SNOWMASS*. In press
130. Rösch, J., Yerle, R. 1983. *Sol. Phys.* 82: 130–50
131. Sabatier, P. C. 1977. *J. Geophys.* 43: 115–37
132. Scherrer, P. H., Delache, P. 1984. In *CATANIA*. In press
133. Scherrer, P. H., Wilcox, J. M. 1983. *Sol. Phys.* 82: 37–42
134. Scherrer, P. H., Wilcox, J. M., Christensen-Dalsgaard, J., Gough, D. O. 1982. *Nature* 297: 312–13
135. Scherrer, P. H., Wilcox, J. M., Christensen-Dalsgaard, J., Gough, D. O. 1983. *Sol. Phys.* 82: 75–87
136. Schmieder, B. 1978. *Sol. Phys.* 57: 245–53
137. Scuflaire, R. 1974. *Astron. Astrophys.* 36: 107–11
138. Scuflaire, R., Gabriel, M., Noels, A. 1981. *Astron. Astrophys.* 99: 39–42
139. Scuflaire, R., Gabriel, M., Noels, A. 1982. *Astron. Astrophys.* 110: 50–53
140. Scuflaire, R., Gabriel, M., Noels, A. 1982. *Astron. Astrophys.* 113: 219–22
141. Severny, A. B., Kotov, V. A., Tsap, T. T. 1976. *Nature* 259: 87–89
142. Severny, A. B., Kotov, V. A., Tsap, T. T. 1984. In *CATANIA*. In press
143. Shibahashi, H. 1984. In *CATANIA*. In press
144. Shibahashi, H., Noels, A., Gabriel, M. 1983. *Astron. Astrophys.* 123: 283–88
- 144a. Shibahashi, H., Noels, A., Gabriel, M. 1984. In *CATANIA*. In press
145. Spiegel, E. A., Unno, W. 1962. *Publ. Astr. Soc. Jpn.* 14: 28–32
146. Staiger, J. 1984. Thesis. Univ. Freiburg, Fed. Rep. Germany
147. Stebbins, R., Wilson, C. 1983. *Sol. Phys.* 82: 43–54
148. Stein, R. F., Leibacher, J. W. 1974. *Ann. Rev. Astron. Astrophys.* 12: 407–35
149. Stein, R. F., Leibacher, J. W. 1981. In *The Sun as a Star*, ed. S. Jordan, pp. 289–300. *NASA SP-450*
150. Tassoul, M. 1980. *Ap. J. Suppl.* 43: 469–90
151. Ulrich, R. K. 1970. *Ap. J.* 162: 993–1002
152. Ulrich, R. K. 1982. *Ap. J.* 258: 404–13
153. Ulrich, R. K., Rhodes, E. J. Jr. 1977. *Ap. J.* 218: 521–29
154. Ulrich, R. K., Rhodes, E. J. Jr. 1983. *Ap. J.* 265: 551–63
155. Unno, W., Osaki, Y., Ando, H., Shibahashi, H. 1979. *Nonradial Oscillations of Stars*. Univ. Tokyo Press. 323 pp.
156. Vandakurov, Yu. V. 1967. *Astron. Zh.* 44: 786
157. van der Raay, H. B., Claverie, A., Isaak, G. R., McLeod, J. M., Roca Cortez, T., et al. 1984. In *CATANIA*. In press
158. Wiggins, R. A. 1972. *Rev. Geophys. Space Phys.* 10: 251–85
159. Willson, R. C., Hudson, H. S. 1981. *Ap. J. Lett.* 244: L185
- 159a. Woodard, M. 1984. *Nature*. In press
160. Woodard, M., Hudson, H. 1983. *Sol. Phys.* 82: 67–73
161. Woodard, M., Hudson, H. 1984. In *CATANIA*. In press
162. Worden, S. P., Simon, G. W. 1976. *Ap. J. Lett.* 210: L163–66
163. Yerle, R. 1981. *Astron. Astrophys. Lett.* 100: L23–25
164. Zahn, J.-P. 1970. *Astron. Astrophys.* 4: 452–61